JOURNAL OF ENGINEERING AND APPLIED SCIENCE, VOL. 67, NO. 8, DEC. 2020, PP. 1995-2012
FACULTY OF ENGINEERING, CAIRO UNIVERSITY

EFFECT OF CRACKS IN WIND TURBINE BLADES ON NATURAL FREQUENCIES DURING OPERATION

A. E. ELDEEB[1], M. E. EL-ARABI[2], AND B. A. HUSSEIN[3]

ABSTRACT

Most publications that are concerned with the crack detection via analyzing Eigenfrequencies or deformation modes of wind turbine blades (WTBs) are done in stationary condition. This paper however proposes a novel approach that could study the effect of WTB cracks during rotation at any speed without the need to stop the turbine by using multibody analysis. This approach will reduce the cost of its maintenance substantially, since it will avoid the cost of downtime for wind turbine during crack detection. This approach considers both the increase in stiffness due to rotation (known as centrifugal stiffening effect), and stiffness reduction due to cracks presence in the blade. This study tests the capability of the proposed approach in detection of location and size of cracks in WTB. A finite element model was built for WTB by using MSC/ADAMS. A parametric study is then applied to the WTB model to study the effect of crack size and crack location on the modal parameters of the WTB. Finally, the combined effect of cracks presence and rotational speed on the modal parameters of the WTB during rotation are also investigated.

KEYWORDS: Wind turbine blade, Crack detection, Dynamic analysis, Finite Element, Centrifugal stiffening effect.

1. INTRODUCTION

The use of wind power increased rapidly in the last years. Horizontal axis wind turbine (HAWT) is designed for a predicted lifetime of about 20 years. However, any defects in the turbine components such as a crack in turbine blade can influence its reliability and cause considerable downtime. Therefore, a blade crack should be detected early before it propagates and causes catastrophic failure in the turbine. The wind turbine

[1] Teaching Assistant, Mechanical Design and Production Department, Faculty of Engineering, Cairo University, Giza, Egypt.
[2] Professor, Mechanical Design and Production Department, Faculty of Engineering, Cairo University, Giza, Egypt.
[3] Assistant Professor, Mechanical Design and Production Department, Faculty of Engineering, Cairo University, Giza, Egypt and Mechanical Engineering Department, Nile University School of Engineering and Applied Sciences, Giza, Egypt, bassam@eng.cu.edu.eg

blades (WTBs) are considered the largest rotary component and they encounter various loads over their lifetime. Besides, the cost of blades represents about 18 % of the total turbine cost [1]. In addition, the repair cost and time of the blades are considered the highest due to their installation at high altitudes and their fabrication from expensive materials [1]. Moreover, any crack in the blade will cause rotating unbalance that will destroy the whole system if this crack was not treated in proper time. Thus, the structural health monitoring of the blades received more attention than other components from many researchers.

Various sensors and techniques are used for crack detection of the WTBs such as Acoustic emission (AE), ultrasonic, shearography, fiber optics, eddy current, *laser* Doppler vibrometer (LDV), and strain gauges [2, 3]. All these sensors and techniques have their advantages and limitations. Also, Vibration-based method witnessed a considerable attention in the recent studies. This technique relies on the alteration in modal parameters due to the crack existence. The physical characteristics of the blade such as stiffness, mass and damping represent the main factors of the modal characteristics such as Eigenfrequencies and mode shapes. The existence of any crack in the blade will cause a reduction in the stiffness. Consequently, the value of natural frequency will be reduced, and the mode shape will be altered. This change in modal parameters is used as an indicator for crack presence in the WTB. The authors in [4] demonstrated the ability of this method for damage detection of the WTB by using short time Fourier transform (STFT). Simulation was applied to a WTB model with reduction in the stiffness of the WTB. It was found that the dominant frequency decreased and the displacement in the flap-wise direction increased during stiffness reduction. The alteration in natural frequencies due to the presence of cracks in the blade of steam turbine was tested in [5]. A 3D model of the blade was built then finite element analysis using ANSYS was applied to the blade. Experimental test was performed to the cracked blade to validate the results of ANSYS tool. They found low variation between the experimental and ANSYS results that are less than 5%.

The damage presence can be demonstrated by measuring the reduction of natural frequencies. However, it is desired to detect the locations, numbers, and sizes of cracks

to simplify damage diagnosis. Mode shapes were used in different studies to identify the cracks presence and detect their locations in the structure. The authors in [6] proved the ability of mode shapes to determine the cracks locations on a WTB.

Curvature mode shape (CMS) was introduced in the recent studies for damage detection. This method can determine damage existence, crack location and crack size. The authors in [7] have incorporated the method of FEA and mode shape difference curvature (MSDC) for crack detection of the WTB. FEA was used to determine whether there is a crack or no based on the reduction in Eigenfrequencies due to damages. While, MSDC was used to detect the cracks locations and determine their severity [7]. The authors in [8] used vibration technique to identify the cracks in a 6.5 m WTB using experimental and numerical methods. They performed operational modal analysis (OMA) experimentally on a healthy and cracked blade using 10 accelerometers. Numerical method was used to define the location of the crack by using CMS that change obviously in the damage region. The difference in CMS between the healthy and cracked blade increases by increasing the damage size. The authors in [9] applied different vibration methods to detect the cracks of 5 MW wind turbine whose blade is 61.5 m. They investigated different modal parameters to detect the blade damage, such as frequency, mode shapes, CMS, modal assurance criterion (MAC), coordinate modal assurance criterion (COMAC), and modal strain energy (MSE). They concluded that frequency, mode shape, MAC and COMAC techniques have small sensitivity to the damage. By contrast, MSE and CMS have high sensitivity to the crack presence.

The authors in [10] used the method of wavelet power spectrum (WPS) and vibration modal analysis to detect the presence of cracks in the WTBs. The WPS was found to be more effective than the FFT spectrum to detect the crack presence in the WTB. Besides, the WPS method was used to detect the crack location in the WTB due to the high variation of WPS amplitude near to the crack location. In [11], the authors introduced vibration to a rotating blade during rotation by an electromagnetic actuator. Then the vibration is collected via accelerometers mounted on the blade. The collected results were used in training an algorithm of crack detection by comparing the healthy

and faulty blade at 43 r/min. Then this algorithm was used in crack detection for the blade at two rotational speeds for WTB; 32 r/min and 43 r/min.

In all the aforementioned publications the used techniques for crack detection in the WTBs are applied in a static condition in which the HAWT is out of operation or during rotation with slight change in speed as in ref. [11]. On contrary, the current paper presents new technique for detecting the cracks in the WTBs during rotation at any rotational speed by using a Multibody dynamics software. This method considers both the centrifugal stiffening effect that increases the values of Eigenfrequencies of a blade due to rotation, besides the stiffness reduction due to crack existence that decreases the values of Eigenfrequencies.

In order to implement the proposed approach in the field. First, Vibration would be introduced to a blade in operation by an electromagnetic actuator, then the reading of the blade vibration would be collected by accelerometers distributed along the blade. Then numerical models for healthy and cracked blade are solved on a multibody dynamics software under the blade actual rotational speed. By comparing the numerical models natural frequency results and measured natural frequency results, one can detect the actual crack size and location. It has to be noted that the results of various crack sizes and locations have to be solved until the natural frequencies of the numerical model converges to the frequencies measured in the field.

The centrifugal stiffening is a phenomenon in which the stiffness of a rotating beam is increased due to centrifugal force that causes tension in beams. Centrifugal stiffening of beams was shown in many publications. The centrifugal stiffening of the nearest shape to blades, which is tapered twisted beams is presented in [12]. Centrifugal stiffening could also be calculated by multibody dynamic software. MSC/ADAMS is a multibody dynamic software that is used in this work for dynamic analysis.

2. MULTIBODY SYSTEM DYNAMICS

In this paper, MSC/ADAMS is used to study the effect of rotational speed and crack presence on the dynamic behavior of the WTB. This software utilizes multibody system dynamics in its analysis. In this study, the WTB is modeled in MSC/ADAMS

by using Floating Frame of Reference (FFR) formulation. Therefore, it is necessary to explain the main types of bodies' definitions in multibody systems with more focus on FFR formulation.

A multibody system is composed of a collection of multiple interconnected flexible and rigid subsystems called substructures, components, or bodies. Each of these subsystems is exposed to considerable amounts of rotational and translational displacements. These subsystems are connected by using various joints. Some examples of mechanical systems are mechanisms, machines, space structures, robotic manipulators, and vehicles. Mostly, the motion of these systems is characterized by nonlinear dynamic equations that are difficult to be solved using analytical methods. These types of dynamic equations are solved widely using numerical methods.

The material motion of subsystems is studied according to three classifications: rigid body, FFR bodies, and continuum mechanics bodies. Rigid body implies that the body deformation is so small, and it does not affect body motion. In a more general representation, the FFR body can perform a small change in its dimensions due to deformation, in addition to large linear displacement and rotational displacement. In space, the FFR body motion is described completely by six general coordinates; in addition to, numerous elastic coordinates that describes its deformation. Continuum mechanics approach targets studying the general very flexible body motion that include large rotation and large deformation. Consequently, the continuum mechanics approach has disadvantages, such as large dimensions and nonlinearity. Therefore, this method requires extensive calculations that lead to very large computational time for complicated structures.

FFR formulation is applied to formulate the flexible bodies' motion. This formulation uses two sets of coordinates that are attached to the flexible body. These two sets of coordinates are named elastic and reference coordinates. Reference coordinate determines the orientation and position of a chosen flexible body reference frame, mostly the center of mass is the origin of this reference frame. While, the body deformation relative to this reference frame is defined by using the elastic coordinate. The method of Rayleigh–Ritz is applied to introduce these elastic coordinates. Any point

on the flexible body can be identified in the global position by using these two sets of coordinates.

As an example of FFR representation, the global position **r** of an arbitrary point on a rigid body can be represented as follows [13].

$$\vec{r} = \overrightarrow{r_0} + A(\overrightarrow{\overrightarrow{u_0}} + \overrightarrow{\overrightarrow{u_f}}) \quad (1)$$

where $\vec{r}_0$ is vector of global position of the origin of the reference frame on the body, which is mostly the body center of mass. The matrix A is the rotation matrix that can be defined as the direction cosines of the body reference frame. The vector $\overrightarrow{\overrightarrow{u_0}}$ is the position vector of the arbitrary point defined in the reference frame of the rigid body. The vector $\overrightarrow{\overrightarrow{u_f}}$ is the vector of displacement of the arbitrary point defined in body reference frame. Figure 1 shows an example a flexible beam represented by FFR.

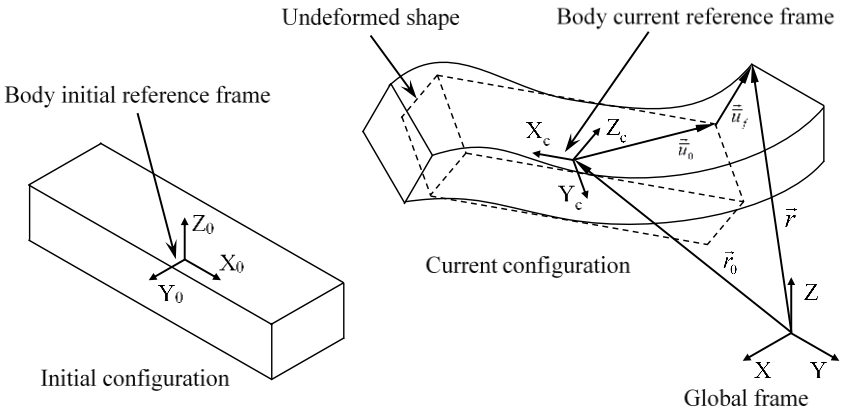

Fig. 1. FFR representation.

The displacement of any arbitrary point can be represented as a sum of the body mode shapes multiplied by the amplitude of each mode during motion. It has to be noted that the mode shapes are represented as a function in the local undeformed position of arbitrary points. FFR formulation focuses on studying small deformation of flexible bodies, therefore it utilizes linearized modes obtained by finite element solution. The modes of selected low frequencies are only included in the resulting model that are based on the assumption of small deformations of flexible bodies [14].

FFR formulation was used in some studies to describe large deformation of flexible bodies. These studies depend on discretizing a flexible body into a set of FFR bodies, each of them experiences a small deformation as shown in Fig. 2. These FFR

bodies are connected by using rigid joints to form together a flexible body that can experience significant deformation.

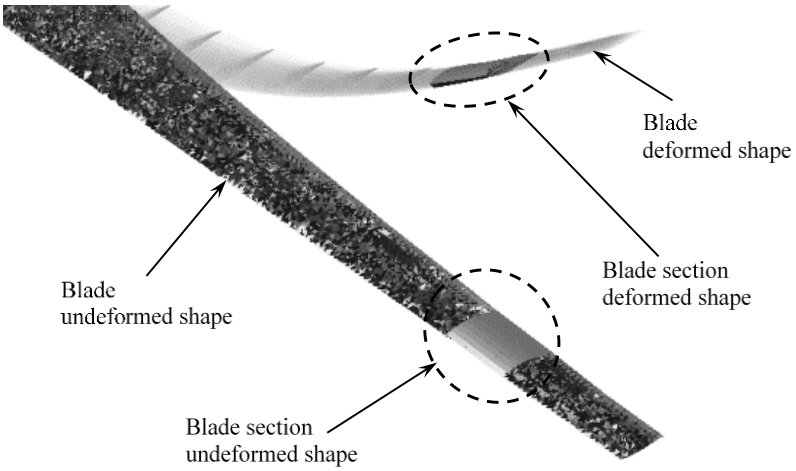

Fig. 2. WTB discretizing to capture large deformation.

The ability of FFR to describe the deformation of flexible bodies for rotating beams was demonstrated in literature [15]. It was shown that FFR can detect the centrifugal stiffening effect at various rotational speeds. Consequently, FFR can be used in the current study that aims to consider the centrifugal stiffening effect.

3. DESIGN OF WTB

The WTB geometry parameters, such as chord length c_r and twist angles β_r are calculated as shown in [16-17]. Then the theory of blade element momentum (BEM) is employed to calculate the aerodynamic forces. NACA 63-415 is the selected airfoil with $Re = 1E6$. The WTB has twenty sections with two sections at the beginning of the blade that are used to connect the WTB to the hub for WT as shown in Fig. 3. Each section is placed at radius *r* from the hub with width *dr* and chord length c_r, while *R* represents the WTB length. The WTB material selected in this study is Aluminum that is commonly used for small size wind turbines, while the rigid hub is made of steel.

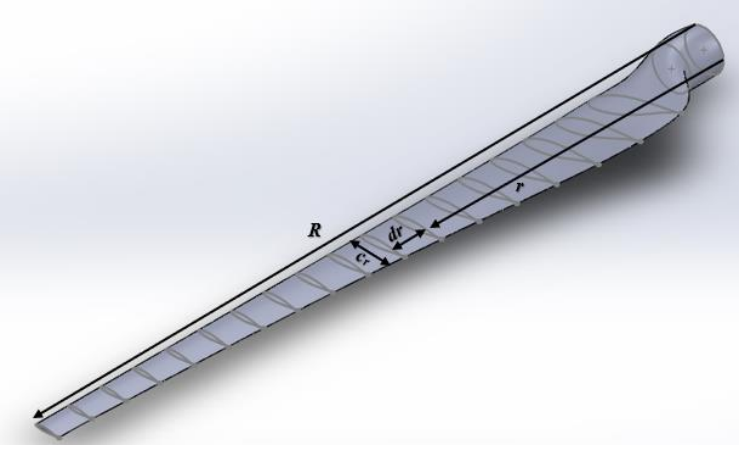

Fig. 3. WTB elements.

3.1 WTB Aerodynamics

The tangential and normal components of aerodynamic forces are derived based on the drag and lift force in addition to the twist angle of the blade. Prandtl's loss tip correction factor (P_{tc}) is used to correct the assumptions of the BEM theory at the blade tip [16-17]. A complete explanation of the steps that are used in the current paper of calculating the normal and tangential components of aerodynamic forces is presented in literature [16-19]. The following specifications were considered for the WTB used in this study: R = 5 m, optimum tip speed ratio is 7.5, optimum angle of attack is 5.25° and optimum lift coefficient is 0.9461.

The aerodynamic forces are calculated at different wind speeds to get various rotational speed for the rotor. Figure 4 shows the calculated aerodynamic forces at wind speeds 5, 10, and 15 m/s versus the WTB elements.

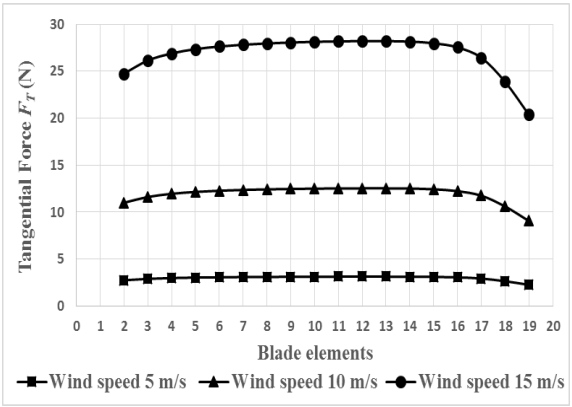

(a) Tangential forces

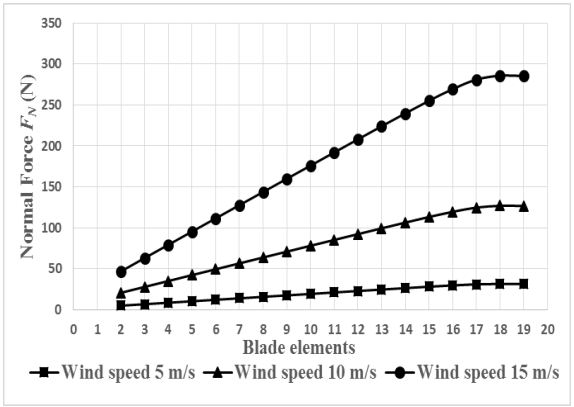

(b) Normal forces

Fig. 4. The calculated aerodynamic forces at different wind speeds versus WTB elements.

3.2 Wind Turbine Power and Torque Control

The power curve of the WTs is illustrated in Fig. 5. From this graph, the operational range of the wind speed is between U_{min} (cut-in) and U_{max} (cut-out) wind speeds. The WT is not operated out of these limits. Below the speed of cut-in, the WT is shut down because the wind speed is not high enough to compensate the losses and operation costs. Above the speed of cut-out, the WT is stopped to prevent structural overload. The power curve in Fig. 5 has two main regions. In region I, the available power increases by increasing the wind speed till it reaches the rated power (P_N) at the rated wind speed (U_N).

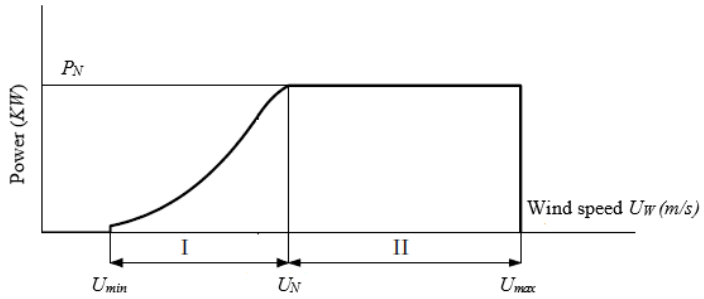

Fig. 5. Wind turbine power curve [19].

This objective is achieved by using variable speed control in this region in which the rotor speed can be controlled through the generator torque. In region II, the main goal is to keep the generated power constant and equal to the rated value to prevent strcutural overloading. This is achieved by using variable pitch control system, so that the WT is operated with constant generator speed and constant rated power [19].

In this paper, the WTB simulation is applied by using MSC/ADAMS within region I in which variable speed control needs to be achieved. The steady state condition in this region is achieved by setting the net torque that affects the system equal to zero. The net torque represents the difference between aerodynamics and generator torque on the blade. The generator torque on the blade is the generator torque on its rotor divided by the WT gearbox speed ratio and number of blades. In the rest of the paper, the generator torque is referred to the resultant torque of the generator on a blade. The aerodynamic torque is calculated from $T_{av} = \frac{1}{2}\pi\rho R^2 C_p V^3 / \omega$.

The generator torque in the commercial WTs with variable speed in region I is set equal to the aerodynamic torque such that $T_{gen} = k\,\omega^2$, where $k = \frac{1}{2\lambda_{op}^3}\rho\pi R^5 Cp_{\max}$ [19-20]. The value of k used in this study is 2.7 N.m.s^2.

3.3 WTB Modelling and Simulation

The WTB modelling is performed by using a CAD software (SolidWorks). The modelling is dependent on the airfoil coordinates that have standard values according to the airfoil type [21]. SolidWorks is used as the preprocessor of geometry for MSC/ADAMS. The airfoil profile is considered as closed curve that consists of collection of points which represent the profile coordinate system. The WTB was divided into nineteen segments to include the high nonlinear deformations, so that MSC/ADAMS can recognize a large deformation during rotation. Each segment was imported from SolidWorks as a rigid body. ADAMS Flex was then used to convert all rigid body segments into flexible ones by using FE. FE mesh was applied with tetrahedral quadratic elements to each segment. The generated flexible bodies were then connected using fixed joints from both sides to act as single body. The WTB was then connected from the root section with the rigid hub by fixed joint. While, the rigid hub was connected with the ground by using revolute joint to permit the rotation around *Z*-axis as shown in Fig. 6.

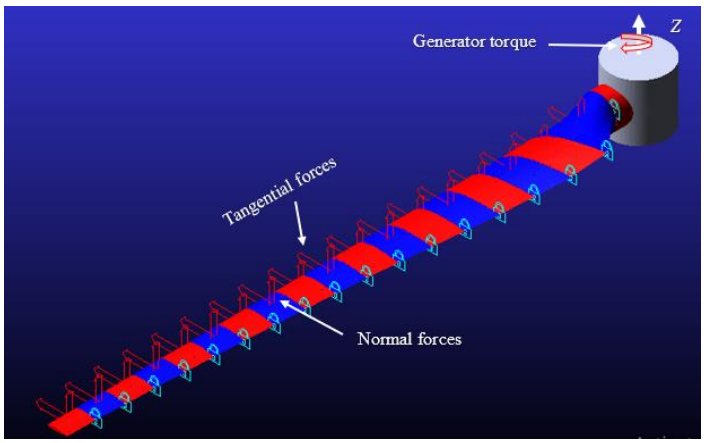

Fig. 6. Applied aerodynamic forces and torque to the WTB model in MSC/Adams.

The actual system of the WT is driven by the aerodynamic forces that affect the WTB. These forces are divided into normal components in the direction of Z axis and tangential components that generate aerodynamic torque around the rotor hub axis. The generator produces torque that resists the aerodynamic torque as explained in previous section. The tangential and normal forces that were obtained in Fig. 4 were added to each WTB element, while the generator torque was applied to the hub at the revolute joint as shown in Fig. 6.

Thus, different rotational speeds of the rotor were obtained by changing the values of tangential and normal forces at different wind speeds as explained before, while the generator torque was kept as a function of rotational speed with constant value for k that was mentioned in section 3.2.

3.4 Variable Speed Control

According to the values presented in the previous section, the blade length R = 5 m, and the wind speed U_w is 5, 10, and 15 m/s, respectively. Then the rotor rotational speed ω at steady state when the aerodynamic torque is equal to the generator torque are, 7.5, 15, and 22.5 rad/s, respectively. It has to be noted that the rotor steady state rotational speed obtained by MSC/ADAMS were very close to these analytical results.

4. RESULTS

4.1 Crack Size Effect

A parametric study was applied to the WTB model using MSC/ADAMS to study the effect of crack size on the Eigenfrequencies in static condition. The generated crack in the WTB model has length (L_c), width (W_c), and depth (D_c) as illustrated in Fig. 7.

The crack is located at 72 % of the blade length measured from the root side, because the most common crack location is between 70 % and 75 % of the blade length [1]. Three cases of crack sizes are investigated that are small, medium, and large. This classification is applied to prove the decrease of Eigenfrequencies by increasing the crack size. Crack of small size has L_c = 50 mm, W_c = 3 mm and D_c = 25 mm. Medium crack size has L_c = 80 mm ,W_c = 5 mm and D_c = 30 mm. While, the large crack size has L_c = 110 mm, W_c = 7 mm and D_c = 35 mm.

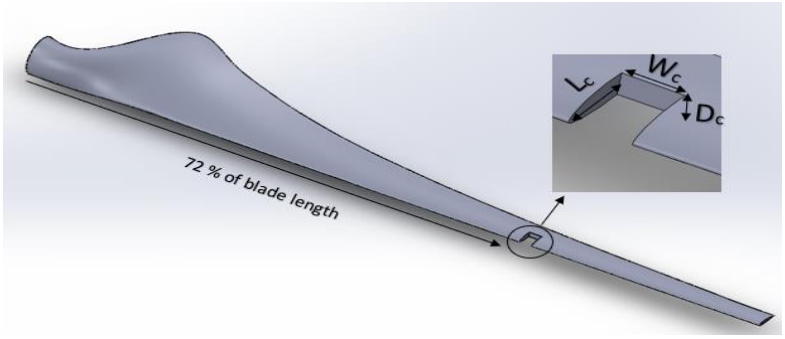

Fig. 7. Crack specifications (not to scale).

The WTB model was subjected to modal analysis to compare the behavior of the blade at zero rotational speed between the healthy and cracked blade. The used numerical integrator in MSC/ADAMS in this analysis was Hilber-Hughes-Taylor implicit formula (HHT) integrator with error tolerance 10^{-8}. The analysis was done for the healthy and the three cases of cracked blade in which small, medium, and large cracks sizes were generated. Figure 8 shows the reduction percentage of Eigenfrequencies for various crack sizes at different vibration modes. The reduction percentage is measured relative to the healthy Eigenfrequencies. It is noticeable that the reduction percentage increases by increasing the crack size in all vibration modes. In addition, mode four has the lowest reduction percentage in all sizes of cracks except the large crack size in which minimum effect belongs to mode one. While, mode five has the highest reduction percentage in all cracks sizes.

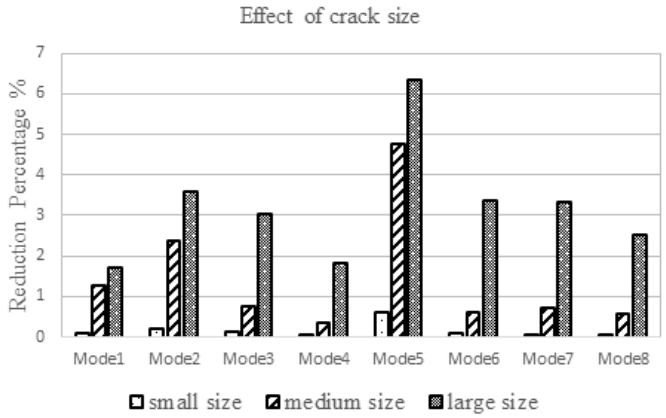

Fig. 8. The effect of various cracks sizes on different modes.

4.2 Crack Location Effect

The effect of crack location on the Eigenfrequencies of the WTB was investigated by using MSC/ADAMS. Medium crack size (L_c = 80 mm ,W_c = 5 mm and D_c = 30) was used in this study. Ten different locations for cracks of equal size are considered along the blade length at equally distance 0.5 m, so that the Eigenfrequencies were investigated due to the presence of each crack individually. Ten simulations were done for each crack location. The used numerical integrator in MSC/ADAMS in the analysis was HHT integrator with error tolerance 10^{-8}. Figure 9 shows the effect of crack location on the Eigenfrequencies of the WTB for different vibration modes. It can be found that most of vibration modes are highly affected with the crack presence after 50 % of blade length measured from the root side. From these results, it is clear that most of modes had the highest reduction in Eigenfrequencies at 70 % of blade length, except modes three and four that had the highest reduction at 50% and 90% of blade length, respectively. The Eigenfrequencies were found to increase due to crack presence nearly at the blade tip. This can be explained as a result that the blade will behave as if its length is shortened and a mass is attached at its tips. As the blade length decrease the blade stiffness will increase, then the Eigenfrequency will increase.

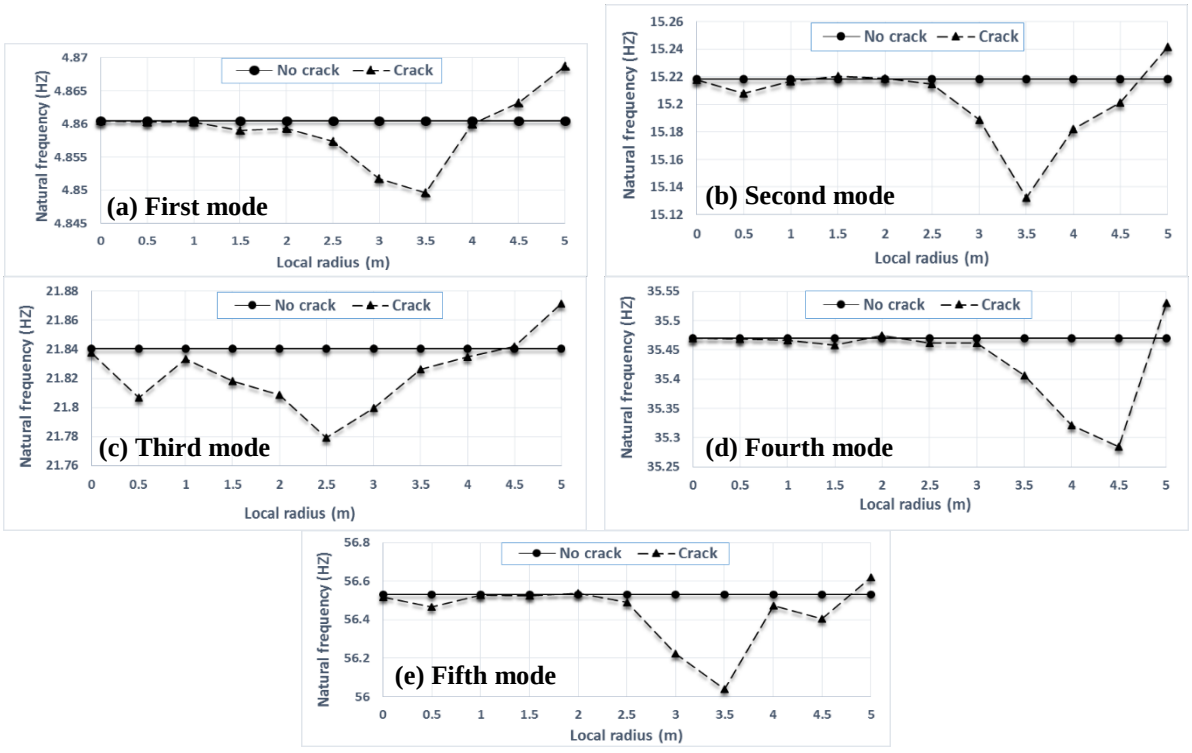

Fig. 9. The effect of the location of crack on the Eigenfrequencies of different modes.

4.3 The Effect of Crack Presence and Rotational Speed

The main goal of this paper is to study the effect of cracks presence and rotational speeds together on the Eigenfrequencies of the WTB during rotation. This section will focus on studying this event. Three cases are investigated in this section, in which large crack size is introduced (L_c = 110 mm , W_c = 7 mm and D_c = 35 mm). First case includes one crack developed at 70 % measured from root section. Second case includes two cracks of the same size that are created at 60% and 70 % of the blade length measured from the root side. Third case includes three cracks of the same size that are created at 60%, 70% and 80% measured from the root section. The simulation time was 200 seconds. The used integrator in the analysis was HHT integrator with error tolerance 10^{-8}. Figure 10 shows the effect of crack presence at different rotational speeds on the Eigenfrequencies of the WTB for the first eight vibration modes.

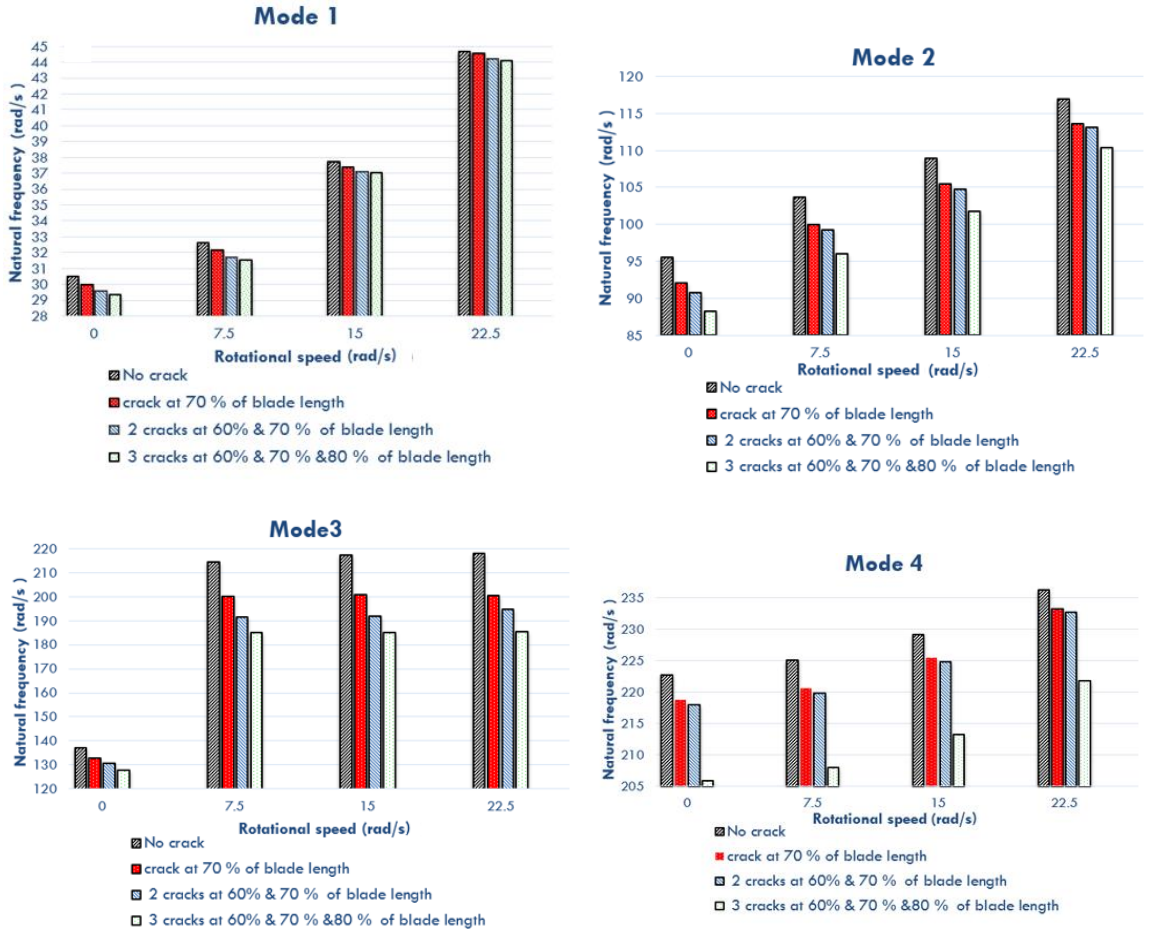

Fig. 10 (a). The effect of different cracks and rotational speed on the Eigenfrequencies of the WTB (modes 1-4).

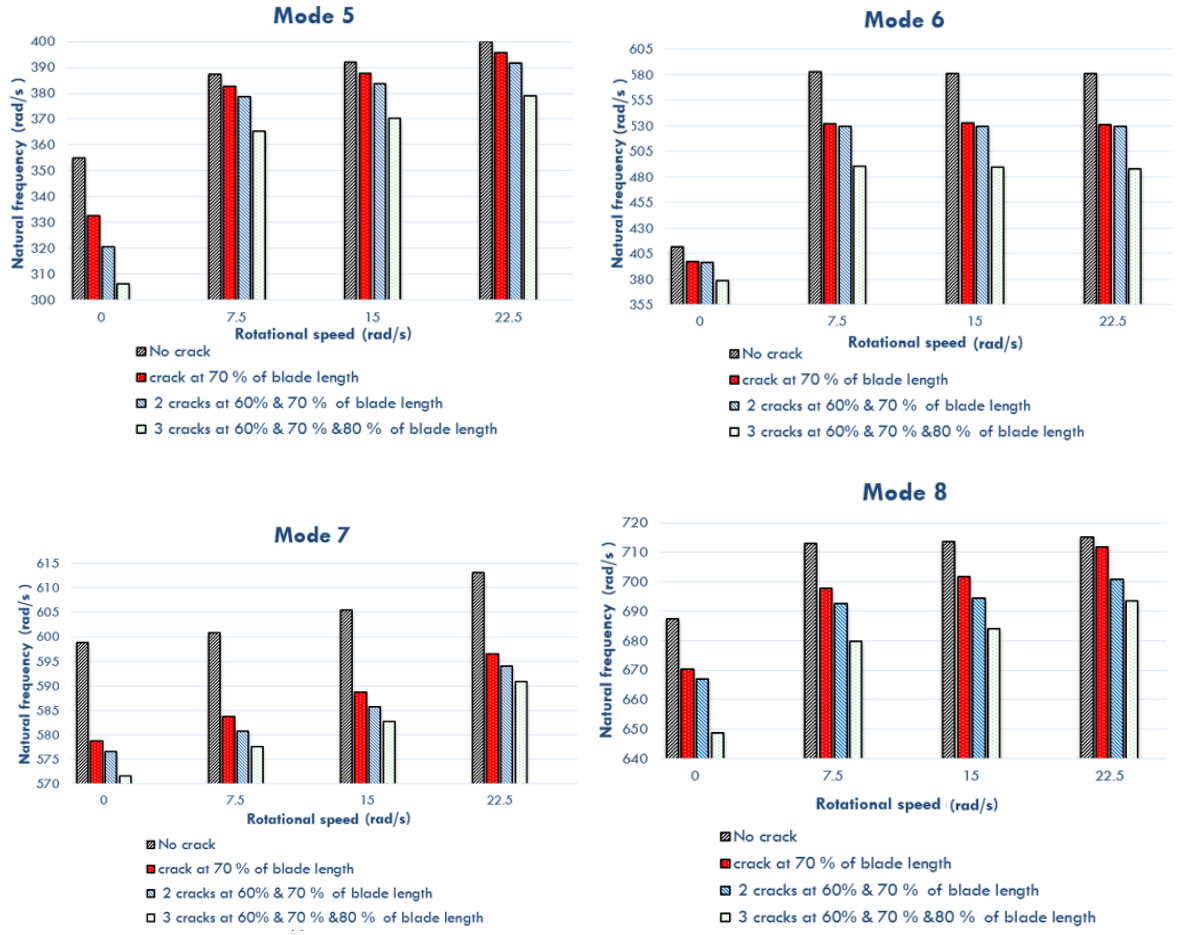

Fig. 10 (b). The effect of different cracks and rotational speed on the Eigenfrequencies of the WTB (modes 5-8).

First mode experienced the centrifugal stiffening effect during rotation, therefore the Eigenfrequencies increased by increasing the rotational speed. By contrast, the reduction in Eigenfrequencies due to crack presence is not significant in this mode. Second mode experienced both effects; the increase in eigenfrequency during rotation and the reduction in Eigenfrequencies due to crack presence. Modes three, six and eight experience a small increase in Eigenfrequencies as a function in rotational speed. While in modes four, five and seven the Eigenfrequency is proportional to the WTB rotational speed. It can be noticed in most cases that the increase in eigenfrequencies due to centrifugal stiffening effect is more than the decrease in them due to cracks. Therefore, centrifugal stiffening effect cannot be ignored when Eigenfrequencies are used in crack detection.

5. CONCLUSIONS

This work presented a new technique for detecting the cracks in the WTBs during rotation without the need to stop the turbine using dynamic analysis software such as MSC/ADAMS. This method considered both the centrifugal stiffening effect and stiffness reduction due to cracks presence in the rotating blade. The centrifugal stiffening effect increases the values of Eigenfrequencies during rotation. By contrast, the presence of cracks in the WTBs reduces the values of Eigenfrequencies due to stiffness reduction.

A WTB model was designed. Aerodynamic forces were calculated based on BEM theory. Different rotational speeds for the rotor were calculated using the analytical equations and they were compared to MSC/ADAMS results. The effect of crack on modal parameters was investigated. The Eigenfrequencies were found to decrease by increasing the crack size. The effect of crack on the Eigenfrequencies was found to be more significant at the higher modes than the lower ones. Different crack locations were investigated. The crack location between 70 % and 80 % of the blade length has the most significant effect on Eigenfrequencies. Finally, the effect of both rotational speed and crack presence on the modal parameters, were investigated. All the vibration modes experienced an increase during rotation due to the centrifugal stiffening effect. Besides, all vibration modes witnessed a decrease due to the crack presence. It was found that, if the centrifugal stiffening is ignored, then the Eigenfrequencies will not indicate a presence crack correctly. The centrifugal stiffening effect was detected at speeds as low as 7.5 rad/s. Thus, centrifugal stiffening effect has to be considered in calculation of blade natural frequencies even for low speed rotors.

DECLARATION OF CONFLICT OF INTERESTS

The authors have declared no conflict of interests.

REFERENCES

1. Ciang, C. C., Lee, J-R., and Bang, H-J., “Structural Health Monitoring for a Wind Turbine System: A Review of Damage Detection Methods”, Measurement Science and Technology, Vol. 19, No. 12, pp.122001-122020, 2008.

2. Li, D., Ho, S. M., Song, G., and Ren, L., Li, H., "A Review of Damage Detection Methods for Wind Turbine Blades", Smart Materials and Structures, Vol. 24, No. 3, pp. 33001-33024, 2015.
3. Yang, R., He, Y., and Zhang, H., "Progress and Trends in Nondestructive Testing and Evaluation for Wind Turbine Composite Blade", Renewable and Sustainable Energy Reviews, Vol. 60, pp. 1225-1250, 2016.
4. Fitzgerald, B., Arrigan, J., and Basu, B., "Damage Detection in Wind Turbine Blades Using Time-Frequency Analysis of Vibration Signals", The 2010 International Joint Conference on Neural Networks (IJCNN), Barcelona, Spain, pp. 1-5, 2010.
5. Shukla, A., Harsha, S. P., "Vibration Response Analysis of Last Stage LP Turbine Blades for Variable Size of Crack in Root", Procedia Technology, Vol 23, pp. 232-239, 2016.
6. Sørensen, B. F., Lading, L., Sendrup, P., McGugan, M., Debel, C.P.; Kristensen, O.J.D.; Larsen, G. C., Hansen, A.M., Rheinländer, J., and Rusborg, J., "Fundamentals for Remote Structural Health Monitoring of Wind Turbine Blades - a Preproject", Riso National Laboratory, Roskilde, Denmark, Technical Report, Risø-R-1336(EN), 2002 .
7. Wang, Y., Liang, M., Xiang, J., "Damage Detection Method for Wind Turbine Blades Based on Dynamics Analysis and Mode Shape Difference Curvature Information", Mechanical Systems and Signal Processing, Vol. 48, No. 1, pp. 351-367, 2014.
8. Lorenzo, E. D., Petrone, G., Manzato, S., Peeters, B., Desmet, W., and Marulo, F., "Damage Detection in Wind Turbine Blades by Using Operational Modal Analysis", Structural Health Monitoring, Vol. 15, No. 3, pp. 289-301, 2016.
9. Rezaei, M. M., Behzad, M., Moradi, H., and Haddadpour, H., "Modal-Based Damage Identification for the Nonlinear Model of Modern Wind Turbine Blade", Renewable Energy, Vol. 94, pp. 391-409, 2016.
10. Abdulraheem, K. F., Al-kindi, G., "Wind Turbine Blade Fault Detection Using Wavelet Power Spectrum and Experimental Modal Analysis", International Journal of Renewable Energy Research, Vol. 8, No. 4, pp. 2167-2179, 2018.
11. Tcherniak, D., and Lasse L. M., "Active Vibration-Based Structural Health Monitoring System for Wind Turbine Blade: Demonstration on An Operating Vestas V27 Wind Turbine", Structural Health Monitoring, Vol. 16, No. 5, pp. 536-550, 2017.
12. Yang, X., Wang, S., Zhang, W., "Dynamic Analysis of a Rotating Tapered Cantilever Timoshenko Beam Based on The Power Series Method", Applied Mathematics and Mechanics, Vol. 38, pp. 1425-1438, 2017.
13. Shabana, A. A., "Dynamics of Multibody Systems", 5th Edition, Cambridge University Press, 2020.
14. Gerstmayr, J., and Schöberl, J. A., "3D Finite Element Method for Flexible Multibody Systems", Multibody System Dynamics, Vol. 15 pp. 4, pp. 309-324, 2006.

15. Nada, A. A., Hussein, B. A., Megahed, S. M., and Shabana, A. A., "Use of the Floating Frame of Reference Formulation in Large Deformation Analysis: Experimental and Numerical Validation", Proceedings of the Institution of Mechanical Engineers Part K Journal of Multi-body Dynamics, Vol. 224 pp. 1, pp. 45-58 2010.
16. Burton, T., Jenkins, N., Sharpe, D., and Bossanyi, E., "Wind Energy Handbook", 2nd edition, John Wiley and Sons, 2011.
17. Tang, X., Peng, R., Liu, X., and Broad, A. I., "Design and Finite Element Analysis of Mixed Aerofoil Wind Turbine Blades", Proceedings of the 7th PhD Seminar on Wind Energy in Europe, Delft, Netherlands, 2011.
18. El Khchine, Y., and Sriti, M., "Tip Loss Factor Effects on Aerodynamic Performances of Horizontal Axis Wind Turbine", Energy Procedia, Vol. 118, pp. 136-140, 2017.
19. Bourlis, D., "A Complete Control Scheme for Variable Speed Stall Regulated Wind Turbines", Fundamental and Advanced Topics in Wind Power, Austria, Vienna, 2011.
20. Chaudhary, U., Mondal, P., Tripathy, P., Nayak, S. K., and Saha, U. K., "Modeling and Optimal Design of Small HAWT Blades for Analyzing the Starting Torque Behavior", 18th National Power Systems Conference, India, 2014.
21. Airfoil database. http://www.airfoiltools.com/. (Accessed 01/5/2020)

تأثير الصدوع في شفرات توربينات الرياح على الترددات الطبيعية أثناء التشغيل

معظم الابحاث المنشورة التي تتعلق بكشف التشقق في شفرات توربينات الرياح عن طريق تحليل التكرارات الذاتية أو أنماط التشوه تتم في حالة ثابتة. على العكس من ذلك، تقترح هذه الدراسة نهجًا جديدًا يمكنه دراسة تأثير شقوق في توربينات الرياح أثناء الدوران باي سرعة دون الحاجة إلى إيقاف التوربينات باستخدام تحليل الأجسام المتعددة. سيقلل هذا النهج من تكلفة صيانت توربينات الرياح بشكل كبير، لأنه سيتجنب تكلفة التوقف عن العمل لتوربينات الرياح أثناء الكشف عن الشقوق. يعتبر هذا النهج كلا من الزيادة في الصلابة بسبب الدوران (المعروف باسم تأثير التقوية بالطرد المركزي)، وتقليل الصلابة بسبب وجود تشققات في شفرات توربينات الرياح. تختبر هذه الدراسة قدرة النهج المقترح في الكشف عن موقع وحجم الشقوق في شفرات توربينات الرياح. تم إنشاء نموذج عنصر محدود لشفرات توربينات الرياح باستخدام برنامج MSC/ADAMS. ثم تم عمل دراسة على انماط التشكل على نموذج شفرات توربينات الرياح لدراسة تأثير حجم الشقوق وموقعها على انماط التشكل. وأخيرًا، تم أيضًا بحث التأثير المشترك لوجود الشقوق وسرعة الدوران.